

Time Reversal and the Neutron

Results of the emiT II Experiment

T.E. Chupp for the emiT II Collaboration

Received: date / Accepted: date

Abstract We have measured the triple correlation $D\langle\mathbf{J}_n\rangle/J_n\cdot(\boldsymbol{\beta}_e\times\hat{p}_\nu)$ with a polarized cold-neutron beam[1,2]. A non-zero value of D can arise due to parity-even-time-reversal-odd interactions that imply CP violation. Final-state effects also contribute to D at the level of 10^{-5} and can be calculated with precision of 1% or better. The D coefficient is uniquely sensitive to the imaginary part of the ratio of axial-vector and vector beta-decay amplitudes as well as to scalar and tensor interactions that could arise due to beyond-Standard-Model physics. Over 300 million proton-electron coincidence events were used in a blind analysis with the result $D = [-0.94 \pm 1.89(stat) \pm 0.97(sys)] \times 10^{-4}$. Assuming only vector and axial vector interactions in beta decay, our result can be interpreted as a measure of the phase of the axial-vector coupling relative to the vector coupling, $\phi_{AV} = 180.012^\circ \pm 0.028^\circ$. This result also improves constraints on certain non-VA interactions.

1 Introduction

The study of time-reversal (T) and charge-parity (CP) symmetry violations has been a subject of keen interest for more than five decades because of its potential to probe many kinds of new physics. The CP-violating parameters of the Standard Model are the CKM phase, which enters in the mixing of three generations of quarks, and the parameter θ_{QCD} . Though all evidence for T and CP violation observed so far in the laboratory can be reproduced by a

The emiT-II Collaboration: T.E. Chupp, R.L. Cooper, K.P. Coulter - University of Michigan, Ann Arbor, MI 48109 USA; S.J. Freedman, B.K. Fujikawa - University of California and Lawrence Berkeley Laboratory, Berkeley, CA 94720 USA; G.L. Jones - Hamilton College, Hamilton, NY 13323 USA; A. Garcia - University of Washington, Seattle, WA 98195 USA; H.P. Mumm, J.S. Nico, A.K. Thompson - National Institute of Standards and Technology, Gaithersburg, MD 20899 USA; C. Trull, F.E. Wietfeldt - Tulane University, New Orleans, LA 70118 USA; J.F. Wilkerson - University of North Carolina, Chapel Hill, NC 27599 USA and Oak Ridge National Lab, Oak Ridge, TN 37831 USA

single number, the phase in the CKM matrix, there is strong evidence that the Standard Model is incomplete. Neutrinos with non-zero masses, the abundance of non-baryonic dark matter, and the baryon asymmetry of the universe are not directly accounted for in the Standard Model. Models of physics beyond the Standard Model that could accommodate these phenomena also generally introduce new CP-violating phases, which could affect T-odd observables in neutron decay. One T-violating observable is the permanent electric dipole moment (EDM) of the neutron [3] or a heavy atom [4,5]; however, the effect of the CKM phase on EDMs is strongly suppressed, and the recent results are considered to tightly constrain θ_{QCD} . The T-odd/P-even triple correlation in polarized neutron decay is uniquely sensitive to the relative phase of vector and axial vector amplitudes, addressing exotic new physics such as leptoquarks [6]. The triple correlation is also sensitive to a combination of scalar, and tensor currents. Though it has been argued that limits on T-odd/P-odd EDM's can be used to place limits on T-odd/P-even interactions and thus on D [7–11], the arguments are based on assumptions that, while reasonable, may not be nature's choice.

Assuming only Lorentz invariance the differential decay rate for polarized neutrons can be written[12]:

$$\frac{dW}{dE_e d\Omega_e d\Omega_\nu} = S(E_e) \left[1 + a \frac{\mathbf{p}_e \cdot \mathbf{p}_\nu}{E_e E_\nu} + b \frac{m_e}{E_e} + \mathbf{P} \cdot \left(A \frac{\mathbf{p}_e}{E_e} + B \frac{\mathbf{p}_\nu}{E_\nu} + D \frac{\mathbf{p}_e \times \mathbf{p}_\nu}{E_e E_\nu} \right) \right]. \quad (1)$$

where $S(E_e) = F(E_e) p_e E_e (E^{max} - E_e)^2$ is the phase space factor with $F(E_e)$ the Fermi-function for $Z = 1$, $\mathbf{p}_e(E_e)$ and $\mathbf{p}_\nu(E_\nu)$ are the momentum (energy) of the electron and neutrino and the neutron polarization $\mathbf{P} = \frac{\langle \mathbf{J}_n \rangle}{J_n}$ is the ensemble average of the neutron spin. The triple-correlation $\langle \mathbf{P} \rangle \cdot (\mathbf{p}_e \times \mathbf{p}_\nu)$ is P-even but odd under motion reversal - the combination of time-reversal and initial/final-state reversal. Thus a non-zero triple correlation can arise from T-violating interactions but also from final state effects. The final-state-interaction contribution for the neutron, approximately 1.2×10^{-5} , can be calculated to 1% or better [14,15]. Neglecting coulomb corrections, the T-violating contribution is

$$D_{\mathcal{T}} \approx \frac{1}{1 + 3|\lambda|^2} \left\{ -2 \frac{\text{Im}(C_V C_A^*)}{|C_V|^2} + \frac{\text{Im}(C_S C_T^* + C_S' C_T'^*)}{|C_V|^2} \right\}, \quad (2)$$

where C_V, C_A, C_S , and C_T are the strengths of vector, axial-vector, scalar and tensor couplings, and $\lambda = |\lambda| e^{i\phi_{AV}} = C_A/C_V$.

The two most recent measurements of D in neutron decay are the original emiT measurement: $D = [-6 \pm 12(stat) \pm 5(sys)] \times 10^{-4}$ [16] and the result from the TRINE experiment at Institute Laue-Langevin: $D = [-2.8 \pm 6.4(stat) \pm 3.0(sys)] \times 10^{-4}$ [17]. A measurement in ^{19}Ne , where the final-state-interactions are an order of magnitude larger than for the neutron, resulted in $D_{^{19}\text{Ne}} = [1 \pm 6] \times 10^{-4}$ [18]. We also note that the R coefficient of the T-odd/P-odd correlation $\sigma_n \cdot (\mathbf{p}_e \times \sigma_e)$ was measured for the neutron [19] and for ^8Li [20], setting constraints on complementary combinations of S and T contributions.

2 Experiment

The emiT experiment took place at the NIST Center for Neutron Research (NCNR). The apparatus, discussed in detail in references [16,21–24], was designed to measure proton-electron coincidences in the decay of neutrons polarized along the axis of an array of detectors and isolate the D -coefficient triple correlation from the T-even-P-odd A- and B-coefficient correlations. The detector array, illustrated in Fig. 1, consists of four electron-detector paddles alternating with four planes of proton detectors arranged in an octagonal geometry concentric with the neutron beam. Electron detectors are 50 cm by 8.4 cm by 0.64 cm thick plastic scintillators with phototubes at either end. An electron event requires coincidence of both phototubes within a timing window of 100 ns. Each of the four proton-detector planes consists of 16 separate proton cells arranged in two rows of eight. After passing through a grounded, 97% transmitting wire mesh, the protons are detected by surface barrier detectors (SBDs), which are negatively biased in the range -25 kV to -31 kV with respect to the decay volume. Focusing by a cylindrical-shell electrode increases the proton-detection efficiency. Within the fiducial volume of the detector array, neutrons are polarized parallel or antiparallel to the magnetic field depending on the spin-flipper state. The magnetic field in the detector had magnitude of approximately 5.6 gauss and was nominally aligned with the neutron beam axis and detector axis.

Data were acquired over a period from October 2002 to November 2003 with some pauses for reactor shut downs and detector maintenance. A total of 934 typically 4-hour runs yields about 316 million good events. Most of the data were taken with nominal proton-acceleration voltages of 28 kV with smaller data sets at 25 kV, 27 kV, and 31 kV. Fig. 2 shows the distribution of all good events as functions of detected proton energy and proton-electron time delay t_{ep} . Good events were determined by a number of cuts on experimental

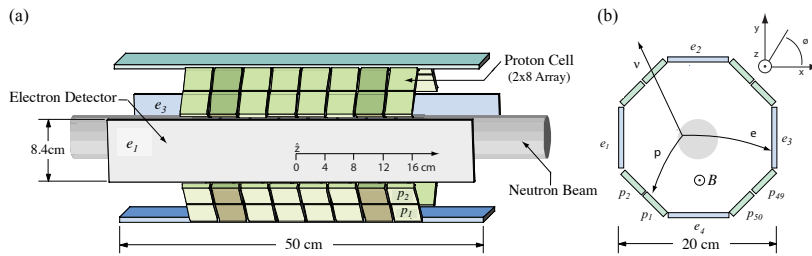


Fig. 1 The emiT-detector array. (a) Side view showing proton-detector planes with 16 proton cells (2×8) in each plane and 50 cm long electron detectors. (b) End view showing the four proton-detector planes and four electron detectors. The magnetic field, directed parallel to the average neutron velocity, causes the proton and electron trajectories to be curved as indicated by the greatly exaggerated paths shown.

parameters including magnetic fields, leakage currents, beta-detector multiplicity, and a software threshold on the beta energy. Background contributions, estimated from the $t_{ep} < 0$ accidental coincidence rate, were subtracted and the counts summed over the window shown. The signal-to-background ratio was approximately 30:1.

The neutron-spin dependence of the count rates, which isolates the correlations given by A , B and D , is given by the difference of rates for spin-up and spin-down neutrons, while the spin independent average of rates includes the beta-neutrino correlation (a term). The spin-flip asymmetry is

$$w^{p_i e_j} = \frac{N_+^{p_i e_j} - N_-^{p_i e_j}}{N_+^{p_i e_j} + N_-^{p_i e_j}} \approx \frac{A\langle\beta_e \mathbf{P} \cdot \hat{p}_e\rangle + B\langle\mathbf{P} \cdot \hat{p}_\nu\rangle + D\langle\beta_e \langle\frac{p_p}{p_\nu}\rangle \mathbf{P} \cdot (\hat{p}_p \times \hat{p}_e)\rangle}{\langle 1 \rangle + a\langle\frac{\hat{p}_e \cdot \hat{p}_\nu}{E_e E_\nu}\rangle + b\langle\frac{m_e}{E_e}\rangle}, \quad (3)$$

where $\mathbf{P}(\mathbf{r})$ is the neutron polarization at a given position and the brackets $\langle \rangle$ indicate that each term is integrated over energies, the neutron beam, and solid angles for proton detector p_i and electron detector e_j . The D -coefficient term is isolated in a difference of w 's that cancels the parity-violating A and B correlations for a uniform, longitudinally polarized neutron beam. For the proton detector p_1 illustrated in Fig. 1:

$$\begin{aligned} v^{p_1} &= \frac{1}{2}(w^{p_1 e_3} - w^{p_1 e_2}) \approx \bar{K}_D P D \\ &+ P \frac{A}{2} [\kappa^{p_1 e_3} \langle \beta_e \cos \theta_e \rangle^{p_1 e_3} - \kappa^{p_1 e_2} \langle \beta_e \cos \theta_e \rangle^{p_1 e_2}] \\ &+ P \frac{B}{2} [\kappa^{p_1 e_3} \langle \cos \theta_\nu \rangle^{p_1 e_3} - \kappa^{p_1 e_2} \langle \cos \theta_\nu \rangle^{p_1 e_2}], \quad (4) \end{aligned}$$

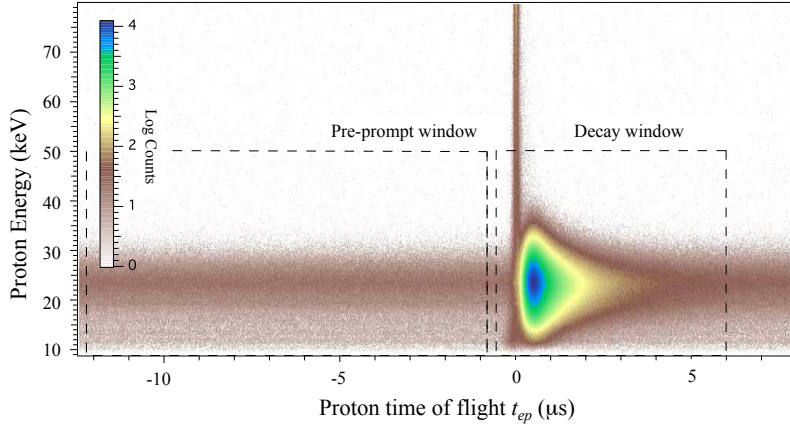


Fig. 2 Detected proton energy vs. proton time-of-flight vs. log of counts for all data. The boxes show the cuts used in the analysis (decay window) and used to determine the random-coincidence background contribution (pre-prompt window).

where $\bar{K}_D = \frac{1}{2}(K_D^{p_1e_3} - K_D^{p_1e_2})$ is an instrumental constant representing the sensitivity to \tilde{D} , and $\kappa^{p_i e_j}$ accounts for the denominator of Eq 3. The terms on the second and third lines in Eq. 4, due to the beta and neutrino asymmetries, are small and enter with opposite sign for adjacent or axially symmetric proton cells for a uniform, longitudinally polarized neutron beam. The small misalignment of the magnetic field leads to an additional contribution to v^{p_i} that cancels in the average of azimuthally opposing proton cells. Thus for uniform beam and polarization, the beta and neutrino asymmetries are cancelled in the average of v^{p_i} when data from 16 proton-cells at the same $|z|$, i.e. $z = \pm 2, \pm 6, \pm 10, \text{ and } \pm 14$ cm for uniform neutron density and polarization, i.e.

$$\bar{v} = \frac{1}{16} \sum_{|z|=const} v^{p_i} = \bar{K}_D P \tilde{D}, \quad (5)$$

where $\bar{K}_D = 0.378 \pm 0.019$ is the average of $K_D^{p_i}$ for the sixteen proton cells determined by Monte-Carlo simulations, and $P = 0.95 \pm 0.05$ is the measured average polarization. Each set of 16 proton cells had the same symmetry as the full detector array, and the experiment thus provided four independent \tilde{D} .

3 Results

A blind analysis was adopted by adding a quantity $K_D^{p_i e_j} \mathcal{B}$ to each $w^{p_i e_j}$ so that when \tilde{D} was extracted from Eq. 5 it was offset from the true value by \mathcal{B} . The factor \mathcal{B} was revealed and subtracted as the final analysis step, after the corrections for systematic errors and all uncertainties were determined.

The principle of the measurement combines v 's from sixteen proton cells that have fairly high efficiency for proton-electron coincidences; however, during the experiment, individual proton cell SBDs did not count for extended periods. Possible variations of the results over time and due to varying experimental conditions were studied by varying the cuts and breaking up the

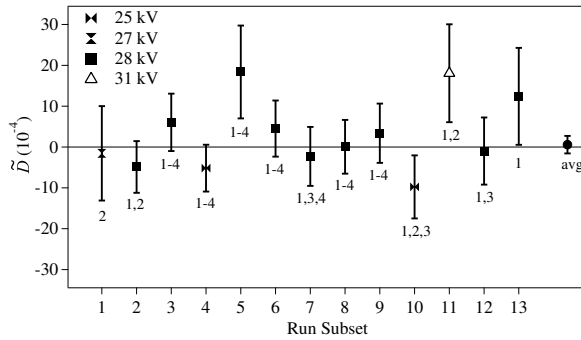


Fig. 3 Results for \tilde{D} by data subset. The proton-acceleration voltage and the proton-detector set included for each subset are indicated. The weighted average of all subsets is 0.58 ± 2.14 with $\chi^2 = 10.44$ for 12 degrees of freedom.

experiment into subsets with roughly equal statistical errors taken under different conditions. Subsets were separated by several possible changes including proton-acceleration voltage, number of live SBDs, and changes to the magnetic field prior to transverse-polarization calibration runs. Due to non-operating SBDs, not all subsets have four sets of 16 proton cells, and the value of \tilde{D} for each data-subset is the weighted average of all available sets of 16 proton cells. The results for the subsets are shown in Fig. 3. A possible correlation of \tilde{D} with high-voltage was revealed in these studies and investigated with data subsets shown in Fig. 3. Testing for a linear correlation had $\chi^2 = 5.6$ for 11 degrees of freedom compared to $\chi^2 = 10.4$ for 12 degrees of freedom assuming no correlation. In addition, the acceleration-voltage dependence of the focusing properties was extensively studied by Monte Carlo showing no effect, and we therefore conclude that the 2.1 sigma slope was an accidental correlation.

When averaged over the entire run, every proton-cell SBD was live for a majority of the time and had a high average efficiency. We can therefore combine counts for the entire run to determine the v^{p_i} 's and to extract \tilde{D} for each set of sixteen proton cells. The results for the four separate \tilde{D} are shown in Fig. 4. The weighted average correcting for $P = 0.95$ and $\bar{K}_D = 0.378$ is $\tilde{D} = (0.72 \pm 1.89) \times 10^{-4}$. This is consistent with the weighted average of all subsets shown in Fig. 3.

The symmetry of the experiment assumed in Eq. 5 was broken by a variety of effects leading to a number of corrections to \tilde{D} . Corrections fall into the main categories: background related including backscattering of protons and electrons, non-uniform efficiencies of the proton and electron detectors and effects related to the asymmetric distribution of the neutron density. The largest corrections and uncertainties a) the effect of high proton-detector thresholds that led to an error in the $w^{p_i e_j}$ due to the unmeasured part of the accelerated proton spectrum leading to a correction on \tilde{D} of $(-0.29 \pm 0.41) \times 10^{-4}$; b) the expansion of the neutron beam, which combined with the 560 μT magnetic field to affect the average of proton-electron angular correlation differently for upstream-downstream proton-cell pairs resulting in a correction of $(-1.50 \pm 0.40) \times 10^{-4}$; c) the coupling of the azimuthal asymmetry of the neutron beam, most strongly influenced by the super-mirror polarizer, to the 6.5 ± 0.4 mrad misalignment of the neutron-beam polarization leading to a correction of $(-0.07 \pm 0.72) \times 10^{-4}$. Corrections were determined using a combination of data, calibration runs that magnified specific systematic effects and Monte Carlo simulations of the experiment, detector geometry and measured neutron beam distribution. A more detailed discussion of all systematic corrections and uncertainties is provided in reference [2]. The total of all systematic corrections is $(-1.68 \pm 1.01) \times 10^{-4}$. When applied to \tilde{D} , our final result is

$$D = [-0.94 \pm 1.89(\text{stat}) \pm 0.97(\text{sys})] \times 10^{-4}. \quad (6)$$

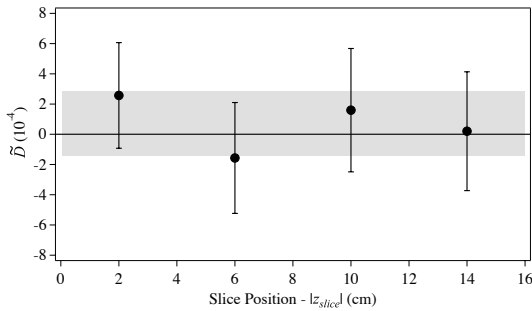


Fig. 4 Results for \tilde{D} for the entire experiment for each set of 16 proton cells. The weighted average is 0.72 ± 1.89 with $\chi^2 = 0.8$ for 3 degrees of freedom.

4 Conclusions

Our result represents the most sensitive measurement of D in nuclear beta decay and can be interpreted in terms of possible extensions of the Standard Model. Assuming no scalar or tensor currents, our result constrains the complex phase between the axial-vector and vector currents to $\phi_{AV} = 180.012^\circ \pm 0.028^\circ$ (68% confidence level). If all currents are allowed there are four additional phases from scalar and tensor amplitudes, which can be constrained under specific assumptions. A more detailed discussion is presented in reference [2].

An improved experiment with the same apparatus would need both more neutron decays and reduced systematic effects. A new beam-line (NGC) under construction at the NCNR and the PF-1 beam at ILL could provide a factor of 10 or more increase of neutron decay rate. Reducing the three major systematic corrections requires eliminating the proton-threshold variations, a more symmetric neutron beam, and smaller magnetic field. The symmetry of the neutron-beam was most strongly affected by the supermirror-bender neutron polarizer, while the $560 \mu\text{T}$ magnetic field was chosen to effect sufficient velocity averaging of transverse-neutron polarization produced in the current-sheet spin flipper. An alternative polarizer is a steady-state polarized ^3He spin filter [25], and the $560 \mu\text{T}$ guide field can be reduced by using an adiabatic-fast-passage neutron spin flipper and effective shimming of the magnetic field along with shielding of external field perturbations. Extending the sensitivity to the level of final-state-effects (10^{-5}) and beyond is a well motivated goal that would require an apparatus with greater geometric efficiency for both proton and electron detectors.

Acknowledgements

The authors gratefully acknowledge informative conversations with Susan Gardner, Wick Haxton, Michael Ramsey-Musolf, and Sean Tulin. The emiT apparatus and emiT-I experiment were developed by many additional collaborators including Shenq-Rong Hwang, Laura Lising, Hamish Robertson, and Tom Steiger along with Bill Teasdale. The neutron facilities used in this work were provided by the National Institute of Standards and Technology, U.S. Department of Commerce. The research was made possible in part by grants from the U.S. Department of Energy Office of Nuclear Physics (DE-FG02-97ER41020, DE-AC02-05CH11231, and DE-FG02-97ER41041), and the National Science Foundation (PHY-0555432, PHY-0855694, PHY-0555474, and PHY-0855310).

1. H.P. Mumm *et al.*, Phys. Rev. Lett. **107**, 102301 (2011).
2. T.E. Chupp, *et al.*, Phys. Rev. C **86**, 035505 (2012).
3. C.A. Baker *et al.* Phys. Rev. Lett. **97**, 131801 (2006).
4. W.C. Griffith Phys. Rev. Lett. **102**, 101601 (2009).
5. M.A. Rosenberry Phys. Rev. Lett. **86**, 22 (2001).
6. P. Herczeg, Progress in Particle and Nuclear Physics **46**, 413 (2001).
7. I.B. Khriplovich, Nucl. Phys. B **352**, 385 (1991).
8. R.S. Conti and I.B. Khriplovich, Phys. Rev. Lett. **65**, 3262 (1992).
9. W.C. Haxton, A. Höring, M.J. Musolf, Phys. Rev. D **50**, 3422 (1994).
10. A. Kurylov, G.C. McLaughlin, M.J. Ramsey-Musolf, Phys. Rev. D **63**, 076007 (2001).
11. J. Ng and S. Tulin, Phys. Rev. D **85**, 033001 (2012).
12. J.D. Jackson, S.B. Treiman, and H.W. Wyld Jr., Phys. Rev. **106**, 517 (1957); J.D. Jackson, S.B. Treiman, and H.W. Wyld Jr., Nucl. Phys. **4**, 206 (1957).
13. B.R. Holstein Phys. Rev. C **28**, 342 (1983); B. Holstein, **Weak Interactions in Nuclei**, p. 166 (Princeton U.P., Princeton, USA) (1989).
14. C.G. Callan and S.B. Treiman, Phys. Rev. **162**, 1494 (1967).
15. S. Ando, J. McGovern, T. Sato, Physics Letters B **677**, 109 (2009).
16. L.J. Lising *et al.* Phys. Rev. C, **62**, 055501 (2000).
17. T. Soldner *et al.*, Phys. Lett. B **581**, 49 (2004).
18. A.L. Hallin, F.P. Calaprice, D.W. MacArthur, L.E. Pilonen, M.B. Schneider, D. F. Schreiber, Phys. Rev. Lett. **52**, 337 (1984); F. Calaprice, in *Hyperfine Interactions* (Springer, Netherlands), Vol. 22. (1985).
19. A. Kozela *et al.*, Phys. Rev. Lett. **102**, 172301 (2009).
20. J. Sromicki, *et al.*, Phys. Rev. C **53**, 932 (1996).
21. H.P. Mumm *et al.*, Rev. Sci. Inst, **75**, 5343 (2004).
22. S. R. Hwang, Ph.D. dissertation, University of Michigan, 1998.
23. L. J. Lising, Ph.D. dissertation, University of California, Berkeley, 1999.
24. H. P. Mumm, Ph.D. dissertation, University of Washington, 2003.
25. T. Chupp *et al.*, Nucl. Inst. and Meth in Physics Res. A **574**, 500 (2007).